New Journal of Physics
The open-access journal for physics

Inhomogeneities in the nonlinear tensorial responses of arrays of gold nanodots

Brian K Canfield[1,4], Hannu Husu[1], Juha Kontio[2], Jukka Viheriälä[2], Tuomo Rytkönen[2], Tapio Niemi[2], Eric Chandler[3], Alex Hrin[3], Jeff A Squier[3] and Martti Kauranen[1]

[1] Optics Laboratory, Institute of Physics, Tampere University of Technology, P O Box 692, FI-33101 Tampere, Finland
[2] Optoelectronics Research Center, Tampere University of Technology, P O Box 692, FI-33101 Tampere, Finland
[3] The Center for Microintegrated Optics for Advanced Bioimaging and Control, Department of Physics, Colorado School of Mines, 1523 Illinois Street, Golden, CO 80401, USA
E-mail: bcanfiel@utsi.edu

New Journal of Physics **10** (2008) 013001 (9pp)
Received 21 September 2007
Published 14 January 2008
Online at http://www.njp.org/
doi:10.1088/1367-2630/10/1/013001

Abstract. We use second- and third-harmonic-generation microscopy to address the tensorial nonlinear responses of individual particles in an array of cylindrical gold nanodots. The responses in both orders exhibit widely-variable, polarization-dependent differences between individual nanodots and thereby indicate tensorial inhomogeneities in the sample. The result provides clear evidence that the second-order response, which is forbidden by symmetry for ideal particles, must arise from small-scale, symmetry-breaking features. A similar result for the third-order response, which is allowed for ideal particles, suggests that both nonlinear responses are dominated by strong variations in field localization around the small-scale features differing among individual nanodots.

[4] Author to whom any correspondence should be addressed.

Contents

1. Introduction

Metal nanostructures offer attractive applications in nanoscale lensing and optical wavelength antennae [1]–[3] as well as magnetic metamaterials [4]. In the metamaterial way of thinking, an individual nanoparticle is considered as an artificial atom whose properties can be designed at will. The collection of such particles then acts as a medium with effective properties, provided that the structural features are sufficiently smaller than the wavelength. However, the plasmonic and magnetic resonances of individual particles depend sensitively on their size, shape and environment. To obtain predictable optical responses and minimize inhomogeneous effects (differences between individual particles), applications depend critically on precise, reproducible fabrication of nanometer-scale features.

Reviews of the recent literature reveal that current fabrication methods such as electron beam lithography (EBL) yield imperfect structures with small defects and deviations from the intended design. These small features may lead to unexpected phenomena already in the linear optical response of the structures, e.g. optical activity or shifted transmission axes [5]–[7].

Small-scale features can act as attractors for intense local fields and can thus influence even more strongly nonlinear responses, which scale with a high power of the field. For example, the second-order response depends strongly on polarization [8] but is also sensitive to small symmetry-breaking features [5, 6]. Theoretical papers predict small-scale polarization dependences in second-harmonic generation (SHG) from rough metal surfaces, describing complicated interactions between overlapping fundamental and second-harmonic fields [9, 10]. Recent experimental work on SHG microscopy of nanostructures supports these findings [11, 12].

The total nonlinear response of an individual nanoparticle therefore depends on a complicated interplay of several factors. A plasmonic resonance is clearly favorable for a strong response [10, 13]. The resonance is associated with a local field distribution containing ‘hot spots’, which arises from the overall features of the structure and may interact either favorably or unfavorably with the locally-varying nonlinearity [14, 15]. Finally, the response from these controllable features interferes with that from the uncontrollable small-scale defects. The relative importance of the various factors may be different for even-order processes, which have a strong noncentrosymmetry requirement and sensitivity to symmetry-breaking defects, and odd-order processes, which are less sensitive to symmetry—for example, third-harmonic generation (THG) [16]. It is therefore of vital interest to examine various

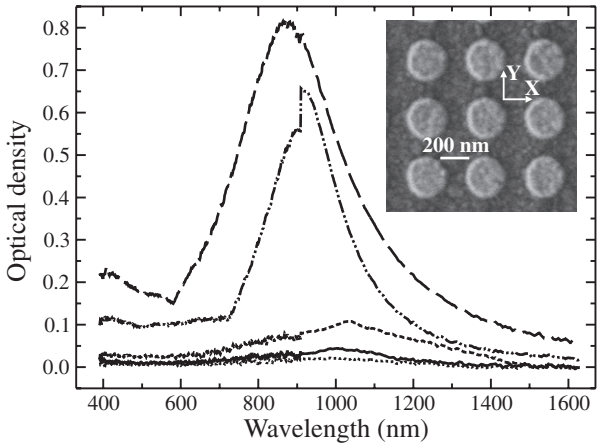

Figure 1. Extinction spectra of 250 nm Au nanodot arrays for different spacings: — — — 400 nm; — ·· — 500 nm (the jump results from spectrometer range overlap); - - - - 1000 nm; —— 1500 nm and ····· 2000 nm. Inset: SEM of 250 nm nanodot array with 400 nm spacing.

polarization-dependent nonlinear optical responses of individual nanoparticles in order to understand the optical processes occurring in metal nanostructures and the relative importance of these factors.

In this paper, we investigate the nonlinear tensorial responses of individual cylindrical Au nanoparticles using both SHG and THG microscopy, allowing us to address individual particles. The results show that both responses vary widely among particles and depend strongly on the polarizations of both the fundamental and signal beams. These dependences indicate different levels and details of symmetry breaking among individual particles, leading to second-order responses that are not expected for ideal particles. However, third-order responses are allowed for them. Our results suggest that both nonlinear responses are dominated by the small-scale features of individual particles through differing distributions of field localization about them.

2. Nanodot samples

Regular arrays of cylindrical Au nanoparticles ('nanodots') 250 nm in diameter were created through nanoimprint lithography (NIL). A master template having a lattice of cylindrical holes was first prepared by EBL on a silicon wafer, then copied to a transparent elastomer stamp [17]. A thin layer of UV-curable NIL resist (Amonil from Amo GmbH) was spin-coated on a prepared fused silica substrate. Nanoimprinting was carried out using the stamp, followed by reactive ion etching, metal deposition consisting of a thin Ti adhesion layer (5 nm) covered by 20 nm of Au to define the vertical nanodot structure, and then the final lift-off processing. The quality of the resulting nanodots was verified by atomic force and scanning electron microscopies (SEMs).

Five different array spacings of 400, 500, 1000, 1500 and 2000 nm were all fabricated on the same substrate. All arrays are square, 500 μm per side. An SEM image from a closely-spaced array in the inset of figure 1 depicts well-defined nanodots in a regular array. To obtain cleanly-separated nonlinear signals from individual nanodots, we focused attention on the array with 1500 nm spacing.

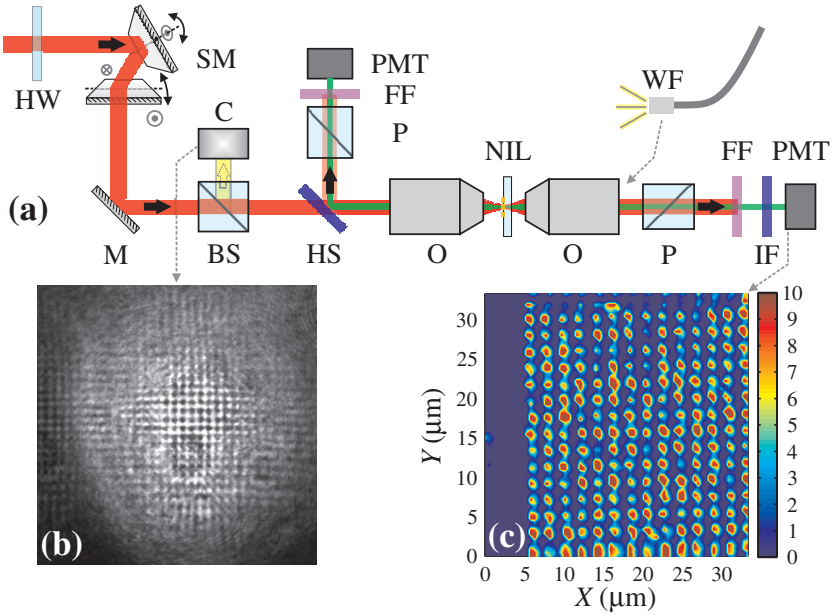

Figure 2. Nonlinear optical microscopy. (a) Experimental set-up. HW: half wave plate; SM: scanning mirrors (the lower mirror rotates out of the plane of the paper); M: turning mirror; BS: beamsplitter; C: CCD camera; HS: harmonic separator; P: polarizer; FF: fundamental-blocking filter; PMT: photomultiplier tube; O: microscope objective; NIL: nanodot sample; WF: white light fiber and IF: interference filter. (b) White light CCD image of array with 1500 nm spacing (contrast enhanced). (c) Transmitted unpolarized SHG example scan of 300 nm-diameter nanodots with 2000 nm spacing.

Unpolarized linear extinction spectra, referenced to the intensity transmitted through the substrate only, were measured using a white light source and a pair of visible and IR fiber optic spectrometers covering 400–1700 nm. The arrays exhibit well-defined spectra with no dichroism as shown in figure 1. Only one extinction resonance per array is observed, indicating that on average the array is highly symmetric along both X- and Y-axes shown in the inset of figure 1. Additional polarized extinction measurements confirmed the existence of only one resonance.

3. Nonlinear optical microscopy

Nonlinear optical microscopy was employed to investigate the nonlinear optical responses of the nanodots. The experimental set-up is depicted in figure 2(a). Illumination at the fundamental wavelength of 1064 nm was provided by a modelocked Nd:glass laser (pulse length 120 fs, repetition rate 100 MHz and average power 50 mW). The beam was linearly polarized and the incident polarization direction was controlled with a half wave plate. Two orthogonally-oriented scan mirrors allowed beam scanning along both X and Y at the sample. The fundamental beam was focused onto the NIL arrays at normal incidence using a moderate numerical aperture microscope objective (NA = 0.65), providing a focused spot diameter at the array of 1 μm full width at half-maximum. Note that higher-NA objectives are intended for optimal function

with cover slips and liquid immersion (not used here), so the experimental conditions were not optimized. The intensity at the focus ($\sim$21 kW cm^{-2}) was well below the damage threshold of the nanodots. Multiple scans of the same area revealed no degradation in signal. The nonlinear responses are also very sensitive to the Z-position of the focused spot. Small positive or negative Z-displacements of 1–2 μm of the nanodots away from the focal region induced rapid declines in signal intensity.

SHG and THG measurements were performed in both transmission (forward) and epi-configuration (backward) directions. In both cases the detector consisted of a polarizer and photomultiplier tube (PMT). In transmission, a second objective (NA = 0.45) collected the light, which then passed through the appropriate harmonic-wavelength interference filter. In epi-configuration, an appropriate harmonic separator (dichroic mirror) was inserted prior to the first objective. The generated epi-harmonic was thus reflected by the harmonic separator into the detection arm as depicted in figure 2(a). A major advantage in epi-configuration, however, is that a lossy interference filter is not required before the PMT, thereby substantially increasing the detected intensity. By rastering the focused spot on the array with the scan mirrors, harmonic intensity as a function of position was recorded. Additional fine adjustment of the sample into the beam focus was accomplished by maximizing the PMT signal.

A secondary detection arm consisting of a beamsplitter and CCD camera located before the harmonic separator was used in conjunction with white light back illumination transmitted through the sample as shown in figure 2(a) for alignment purposes. For the larger array spacings, the regularity of the array can be readily observed with diffraction of the white light, as seen in figure 2(b) for 1500 nm spacing. The pattern is useful for proper XY alignment of the array, and the image sharpness aids in rough Z-positioning of the sample at the beam focus.

Figure 2(c) shows an example of a transmitted SHG scan from an array of 300 nm diameter nanodots with 2000 nm spacing using unpolarized detection. The array's edge is clearly seen on the left, indicating very good contrast between the glass substrate and Au nanodots. Individual nanodots are readily distinguished. Although some variations in their responses are visible, polarized detection is necessary to investigate the tensorial nature of the SHG responses of individual nanodots.

4. Microscopy results

The experimental configuration provides four distinct permutations of pure input and output polarizations, corresponding to the in-plane SHG (THG) tensor components XXX (XXXX), XYY (XYYY), YXX (YXXX) and YYY (YYYY), where the first index refers to the output polarization, and the remaining indices describe the input polarization. At normal incidence, an ideal cylindrical nanodot appears centrosymmetric, and all second-order optical responses are forbidden by symmetry [8]. For third-order, considering an ideal nanodot to be isotropic, then only those tensor components with even numbers of equal indices are non-zero [8], specifically XXXX and YYYY.

At 1500 nm spacing, the nanodots were cleanly separated in the scans. Transmitted SHG responses were measurable—cf figure 2(c)—but THG in transmission was found to be too weak as a result of loss through the interference filter. Epi-SHG and epi-THG scans, on the other hand, provided much stronger signal levels. Polarized epi-SHG results are shown in figure 3.

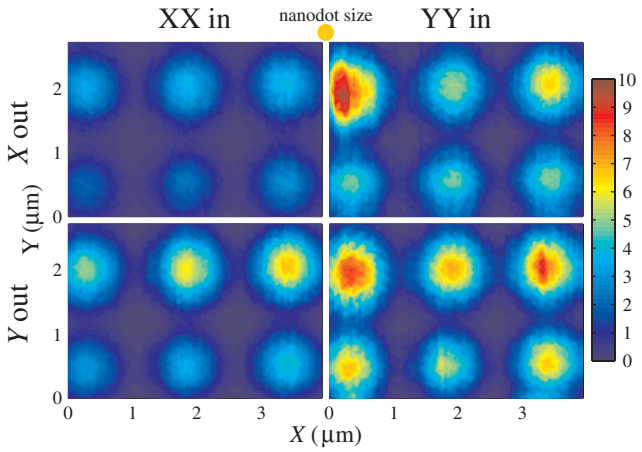

Figure 3. Epi-SHG microscopy scans of Au nanodots using the polarizations indicated.

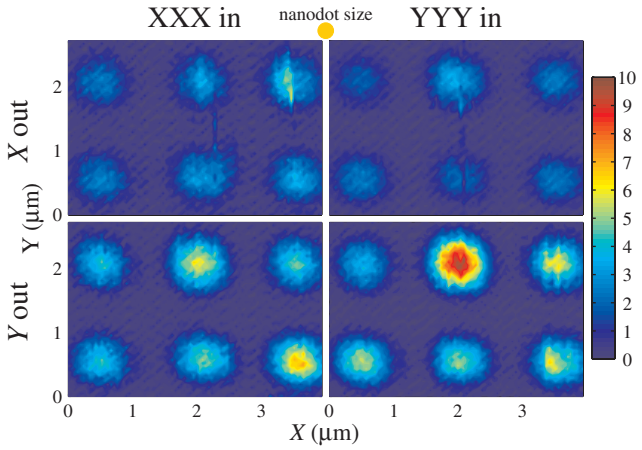

Figure 4. Epi-THG microscopy scans of the same Au nanodots as in figure 3 using the polarizations indicated.

The active response areas appear much larger than the actual 250 nm nanodots (relative size shown) due to their interaction with the much larger 1 μm beam spot. The signal levels were calibrated according to the polarization-dependent system throughput. The background (PMT dark count) has been subtracted from each data set and the intensity then normalized by the resulting maximum among the four plots.

As figure 3 shows, not only do we obtain robust SHG responses from the nanodots, but there are clearly strong polarization dependences even among individual nanodots. SHG is extremely sensitive to both polarization and symmetry, and these results indicate that, despite their well-formed appearance in the SEM inset of figure 1, the nanodots are not ideal [5]. Indeed, close inspection of the SEM shows that some nanodot perimeters are not particularly circular. The nanodots most likely also possess other small defects, on the order of a few nm to a few tens of nm, such as uneven or sloping surfaces.

The epi-THG results in figure 4 are even more intriguing (the same normalization scheme as in figure 3 is used here again). One nanodot (upper row middle) responds most strongly

to YYYY but weakly to XXXX. For ideal symmetry these components should be equivalent. The symmetry-forbidden mixed components XYYY and YXXX also show very interesting behavior. The same nanodot that has a strong YYYY but weak XXXX response also responds strongly to YXXX. However, none of the nanodots exhibit strong XYYY THG responses. The vertical smears appearing in the XXXX and XYYY plots are artifacts of the data collection process.

5. Discussion

The results of the SHG and THG microscopy scans reveal unexpected polarization-dependent behavior from individual nanodots. Several issues regarding the experiments have been addressed. First, we note that tight focusing may lead to complicated and spatially-varying vectorial field distributions within the focal volume and could thereby influence the state and purity of polarization at the sample [18, 19]. However, the $\sim$1 μm spot diameter which results from the 0.65 NA objective does not represent especially tight focusing, so any Z-component polarization, which has a tendency to cancel even in a tight focus, is likely to remain weak. Although such a component could exert minor influences on the nonlinear responses by coupling to the surface normal direction of the samples, we emphasize that the same spot illuminates all the nanodots in each scan, so relative differences among the responses of individual nanodots cannot be attributed to the beam polarization.

Moreover, this choice of NA provides a relatively large-area (compared to the nanodot size), smooth intensity profile that allows us to illuminate individual nanodots uniformly without exciting neighboring nanodots. We also avoid edge effects from the perimeters of the nanodots with this uniform illumination. Strong edge contributions would appear as intense, separated double peaks bordering the nanodot, but these are not observed in figures 3 and 4. The distribution of the local field along the perimeter of a gold nanoparticle has been shown to play a critical role in the enhancement or suppression of SHG [15]. In such cases, a tight focus may play a more important role in exciting edge effects that are avoided here. Furthermore, different nanodot responses would appear more similar if edge effects dominated the responses.

Although the experiments performed here were done for pure input/output polarization combinations, additional information about the nonlinear susceptibility tensors may be obtained from further studies using intermediate polarization angles. However, we note that as the choice of coordinate axes is arbitrary, the detection of any SHG signal alone indicates that small-scale features which break the symmetry exist in individual nanodots. Furthermore, because the responses of individual nanodots exhibit unique polarization dependences, each nanodot has different defects and thus possesses a unique nonlinear response tensor. Small defects tend to localize and enhance the fields in their vicinity, enhancing in turn the nonlinear responses through the resulting high field strengths [9, 10, 14]. However, depending on the local field distribution symmetry, SHG may be either enhanced of suppressed against expectations [15].

In the case of THG, for which not all signals are restricted by the sample symmetry, the variations in the responses between individual nanodots and the presence of symmetry-forbidden signals indicate that the THG response is also driven by these small features. The differences in the THG polarization responses show that, similar to the SHG case, each nanodot possesses a unique nonlinear tensor response for third-order as well. The total macroscopic optical response of an array is therefore comprised of a complicated multitude of individual nanoscopic responses averaged together.

We note that the results presented here apply only to the samples studied and their inherent small features. Other samples, which would possess their own unique distributions of small defects, may behave differently, according to the number and type of the features. However, these results clearly show that small, symmetry-breaking features in metal nanostructures exert strong influences on their optical responses, and that these influences must be considered and characterized in detail for any potential applications.

6. Conclusion

To summarize, we have employed nonlinear optical microscopy to investigate the nonlinear optical tensorial responses of individual Au nanodots. SHG signals from ideally centrosymmetric nanoparticles, for which the second-order response should vanish by symmetry, were detected. THG responses, which are allowed by symmetry, were also observed, even for disallowed polarization combinations. These responses were found to be strongly polarization-dependent and varied widely among individual nanodots, indicating that small symmetry-breaking features are present and scattered among the nanodots, and that they dominate the nonlinear responses. With further optimization, this method also suggests a viable, rapid means of characterizing nanoparticle quality on the scale of an entire array.

Acknowledgments

B K Canfield is currently with the University of Tennessee Space Institute, Tullahoma, TN, USA. This work was supported by the Academy of Finland (nos 114913 and 113245), the Finnish Funding Agency for Technology and Innovation (no. 40321/05 Nanophotonics), the Nanophotonics Research and Development Program under the Ministry of Education of Finland, by NREL subcontract no. ZCO-7-77379 and DOE Prime Contract no. DE-AC36-99GO10337. The NIL master was purchased from Chalmers University of Technology, Göteborg, Sweden. We thank T Furtak and C Durfee for useful discussions.

References

[1] Mühlschlegel P, Eisler H J, Martin O J F, Hecht B and Pohl D W 2005 *Science* **308** 1607–9
[2] Liu Z, Steele J M, Srituravanich W, Pikus Y, Sun C and Zhang X 2005 *Nano Lett.* **5** 1726–9
[3] Sundaramurthy A, Schuck P J, Conley N R, Fromm D P, Kino G S and Moerner W E 2006 *Nano Lett.* **6** 355–60
[4] Enkrich C, Wegener M, Linden S, Burger S, Zschiedrich L, Schmidt F, Zhou J F, Koschny T and Soukoulis C M 2005 *Phys. Rev. Lett.* **95** 203901
[5] Canfield B K, Kujala S, Jefimovs K, Turunen J and Kauranen M 2004 *Opt. Express* **12** 5418–23
[6] Canfield B K, Kujala S, Kauranen M, Jefimovs K, Vallius T and Turunen J 2005 *Appl. Phys. Lett.* **86** 183109
[7] Canfield B K, Kujala S, Laiho K, Jefimovs K, Vallius T, Turunen J and Kauranen M 2006 *J. Nonlinear Opt. Phys. Mater.* **15** 43–53
[8] Boyd R W 1992 *Nonlinear Optics* (San Diego: Academic)
[9] Stockman M I, Bergman D J, Anceau C, Brasselet S and Zyss J 2004 *Phys. Rev. Lett.* **92** 057402
[10] Beermann J, Bozhevolnyi S I and Coello V 2006 *Phys. Rev.* B **73** 115408
[11] Jin R, Jureller J E, Kim H Y and Scherer N F 2005 *J. Am. Chem. Soc.* **127** 12482–3
[12] Zavelani-Rossi M *et al* 2007 *CLEO/QELS and PhAST 2007 Technical Digest* (Washington, DC: Optical Society of America) QFA5

[13] Canfield B K, Kujala S, Kauranen M, Jefimovs K, Vallius T and Turunen J 2005 *J. Opt. A: Pure Appl. Opt.* **7** 110–7
[14] Bozhevolnyi S I, Beermann J and Coello V 2003 *Phys. Rev. Lett.* **90** 197403
[15] Canfield B K, Husu H, Laukkanen J, Bai B, Kuittinen M, Turunen J and Kauranen M 2007 *Nano Lett.* **7** 1251–5
[16] Shcheslavskiy V I, Saltiel S M, Faustov A R, Petrov G I and Yakovlev V V 2006 *Opt. Lett.* **31** 1486–8
[17] Schmid H and Michel B 2000 *Macromolecules* **33** 3042–9
[18] Richards B and Wolf E 1959 *Proc. R. Soc.* A **253** 358–79
[19] Scully M O and Zubairy M S 1991 *Phys. Rev.* A **44** 2656–63